

Excitation Functions for Radioactive Isotopes Produced by Protons below 60 MeV on Al, Fe, and Cu†

I. R. WILLIAMS AND C. B. FULMER

Oak Ridge National Laboratory, Oak Ridge, Tennessee

(Received 15 May 1967)

Cross sections were measured for the production of radioactive isotopes by proton-induced reactions in natural aluminum, iron, and copper at bombarding energies of 60 MeV and lower. Most of the induced activities with half-lives of greater than 1 h were recorded. Cyclotron-accelerated protons were used to bombard stacked foils which were subsequently individually analyzed for their γ radiation with a Ge(Li) spectrometer. Cross sections predicted from an evaporation theory and from cascade-evaporation theory were compared with experimental values; reasonable agreement was obtained.

I. INTRODUCTION

ONLY a few excitation functions of proton-induced radioactivity in aluminum, iron and copper have been previously reported. The development of the lithium-drifted germanium spectrometer, with energy resolution of a few keV, makes more convenient the study of complex γ ray spectra. Therefore, as part of a continuing study^{1,2,3} of residual radiation that can be induced by energetic charged particles, it was decided to measure the intensity and type of radioactivity produced by protons of different energies incident on aluminum, iron, and copper. Knowledge of excitation functions is important because their profiles can yield some information about reaction mechanisms, they give information about residual radiation in the proximity of particle accelerators, and they contribute to the knowledge of the interaction of primary cosmic rays (which are $>80\%$ protons) with matter.

II. EXPERIMENTAL PROCEDURES

The method employed was the stacked-foil technique.⁴ All the foils of Al, Fe and Cu were 2-in. square and from 0.005 to 0.02-in. thick. The foils were cleaned with an organic solvent to insure that the surfaces were free of impurities. A spectrochemical analysis of a sample of the iron foil indicated impurity concentrations of less than 0.2%. Foils stacks of sufficient total thickness to stop the protons were exposed at normal incidence to beams of ~ 60 - or ~ 40 -MeV protons from the Oak Ridge Isochronous Cyclotron. The beams were focused to a 0.5-in. diam. spot in the center of the targets. The target holder was electrically insulated and used as a Faraday cup to record, with an accuracy of $\pm 1\%$, the total charge deposited by the protons. Integrated beams of $\sim 10^{14}$ protons were used.

After bombardment, γ spectra of each foil were measured with a 6-cm³ Ge(Li) spectrometer. A Tennelec

(TC 120) field-effect transistor preamplifier was used. The energy resolution was 9 keV full width at half maximum (FWHM) at 570 keV. The calibration of the spectrometer⁵ permitted both γ energy and peak intensity measurement. The γ spectra were analyzed with a 20 000-channel Victoreen pulse height analyzer used in a 20 \times 1000 mode. The data were read out onto magnetic tape, listed by computer, and graphed by a Cal Comp plotter.

Each spectrum and data list was used to measure the number of counts per unit time in the total effects peaks (mostly photoelectric interaction). All peaks, except that produced by the 511-keV positron annihilation, were identified as due to prominent γ rays from the various isotopes. Except for spectra obtained from aluminum, no attempt was made to identify nuclides by positron annihilation radiation. No peaks that could conceivably have been due to impurities were noted. The absolute detector efficiency⁵ and decay-scheme data⁶ were used to convert peak intensity to source strength of each radioisotope. These data, foil thickness, and beam current measurements were used to calculate production cross sections for all isotopes observed in each foil. The beam intensity was assumed to be attenuated by a geometric total reaction cross section corresponding to a nuclear radius parameter of 1.5 F.

The energy of protons after they had traversed half the thickness of each target wafer was computed from range-energy tables.⁷ The uncertainty of proton energy for each data point is due to energy spread of the incident beam (which was 0.5 MeV FWHM) and to energy-loss straggling. The latter was obtained from tabulated Vavilov distributions.⁸ This straggling for a particular wafer depended on the depth of that wafer in the stack. The energy loss straggling for monoenergetic 60-MeV protons was 0.25 MeV FWHM in the first iron

⁵ R. J. Fox, I. R. Williams, and K. S. Toth, Nucl. Instr. & Methods 35, 331 (1965).

⁶ *Nuclear Data Sheets*, compiled by K. Way *et al.* (Printing and Publishing Office, National Academy of Sciences—National Research Council, Washington, D. C.), 5, Set 1 (1962).

⁷ *dE/dx* and Range Energy Computer Program, H. Bichsel, Tech. Rept. No. 3, Physics Department, University of Southern California, 1961 (unpublished).

⁸ S. M. Seltzer and M. J. Berger, Natl. Acad. Sci.—Natl. Res. Coun. Publ. 1133, Nucl. Sci. Series Rpt. No. 39 (1964).

† Research sponsored by the U. S. Atomic Energy Commission under contract with the Union Carbide Corporation.

¹ K. S. Toth, C. B. Fulmer, and M. Barbier, Nucl. Instr. Methods 42, 128 (1966).

² C. B. Fulmer, K. S. Toth, and M. Barbier, Nucl. Instr. Methods 31, 45 (1964).

³ I. R. Williams and C. B. Fulmer, Phys. Rev. 154, 1005 (1967).

⁴ E. O. Lawrence, Phys. Rev., 47, 17 (1935).

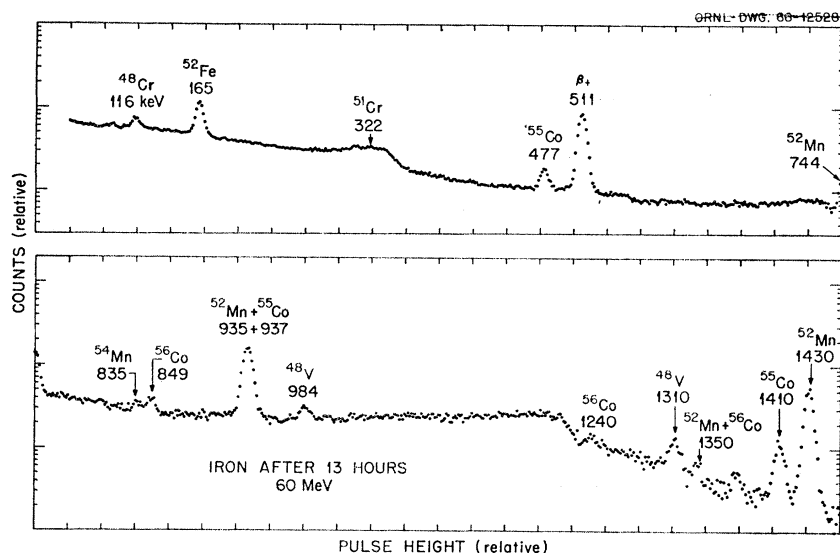


FIG. 1. γ -ray spectrum of the radiation induced in natural iron by 60-MeV protons.

foil, but 1.05 MeV in the foil where the protons had been slowed to 30 MeV. It was for this reason that bombardments were also made with 40-MeV protons. Consequently, the energy uncertainties for the data range from ± 0.35 to ± 0.55 MeV.

TABLE I. γ rays and branching ratios employed in absolute intensity calculations. All the internal conversion coefficients were taken to be zero.

Isotope	Half-Life	Radiation (keV)	Branching Ratio (%)
Aluminum target			
^7Be	53 days	478	12
^{18}F	110 min.	511 (β^+)	200
^{22}Na	2.6 yrs.	1280	100
^{24}Na	15 h	1370	100
Iron target			
^{48}V	16 days	984	100
		1310	100
^{51}Cr	27.8 days	322	9
^{52}Mn	5.7 days	744	82
		935	84
		1430	100
^{52}Fe	8.3 days	165	100
^{54}Mn	314 days	835	100
^{56}Co	18 h	477	24
		511 (β^+)	200
		1410	24
^{56}Co	77 days	849	100
		1240	70
Copper target			
^{61}Ni	37 h	1370	86
^{57}Ni	270 days	122	9.3
^{57}Co		136	0.7
^{58}Co	71 days	805	98
		810	1.6
^{60}Co	5.3 yrs.	1170	100
		1330	100
Copper target			
^{61}Cu	3.3 h	284	10.5
		660	12
^{62}Zn	9.3 h	590	22
		547	
^{66}Zn	245 days	1114	45

Spectra from foils beyond the maximum range of the protons indicated that contributions by reactions induced by secondary neutrons could be neglected.

Sufficient data were taken so that measurements were made at less than 5% increments in proton energy, and at time intervals suitable for identifying the isotopes by half life as well as γ energy.

III. RESULTS AND DISCUSSION

A representative example of the γ -ray spectra obtained in this work is shown in Fig. 1. This spectrum was taken 13 h after bombardment of iron. The median proton energy in this foil was 60 MeV. γ rays from the decay of eight isotopes can be identified, in addition to the 511-keV annihilation quanta from numerous positron emitters. Table I lists the isotopes, their half lives and characteristic radiation.⁶ Figure 2 shows the spectrum of γ rays from a foil deeper in the stack in which the median proton energy was 34.0 MeV. There are fewer γ -rays, indicating that the proton energy is below the threshold for the production of some isotopes. Table II lists Q values for the nuclear reactions of lowest threshold energies that can produce the isotopes.

Excitation functions which have been previously measured by other workers⁹⁻¹² are graphed in Fig. 3. Curves *A*, *B*, *K*, *L*, *M* and *N* are self-explanatory, curves *E*, *F* and *G* are different measurements of the production of ^{22}Na from ^{27}Al , curves *H* and *J* are the results of separate determinations of the cross sections for the production of ^{24}Na from ^{27}Al . It is noted that rather

⁹ F. K. McGowan, W. T. Milner, and H. J. Kim, Oak Ridge National Laboratory No. ORNL-CPX-1 and 2, 1964 (unpublished).

¹⁰ D. B. Smith, Los Alamos Laboratory Report No. LA-2424, 1961, (unpublished).

¹¹ M. Furukawa, S. Kume, and M. Ogawa, Nucl. Phys. 69, 362 (1965).

¹² R. H. Lindsay, Phys. Rev. 147, 792 (1966).

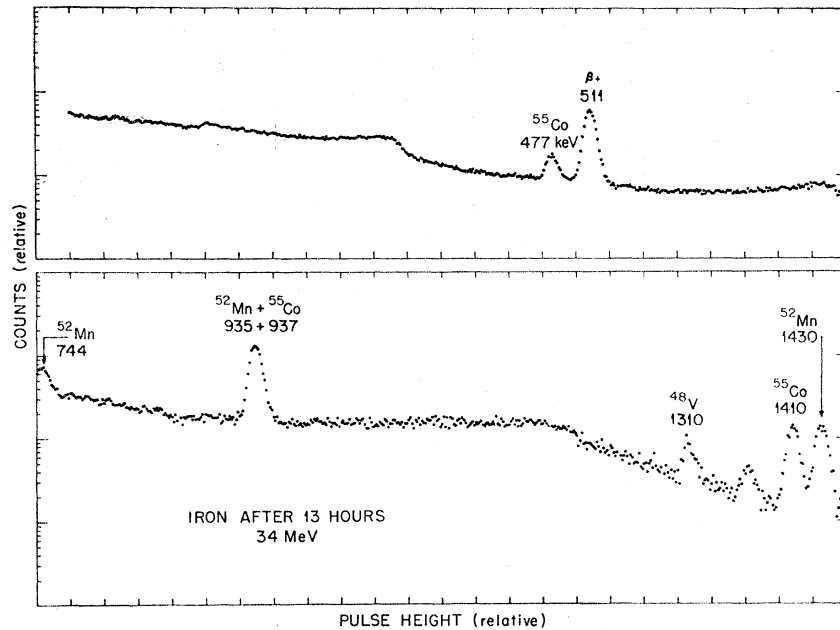


FIG. 2. γ -ray spectrum taken 13 h after bombardment of natural iron by 34-MeV protons.

large differences exist in the two measurements of the cross sections for production of ^{24}Na in aluminum.

Figure 4 shows the excitation function drawn as a continuous line, for the production of 71-day ^{58}Co by protons incident on natural copper. The scatter of data points is typical for the work reported here. As seen from the graph the threshold for the reaction is 29 ± 3

MeV; by comparison with Table II of threshold energies calculated using the mass table of Mattauch, Thiele and Wapstra¹³ it is possible to conclude ^{58}Co is not produced with appreciable cross section from the more abundant copper isotope by the reaction $^{63}\text{Cu}(p,\alpha)^{58}\text{Co}$.

Figure 5 shows the excitation functions for the production of additional radioisotopes by protons interact-

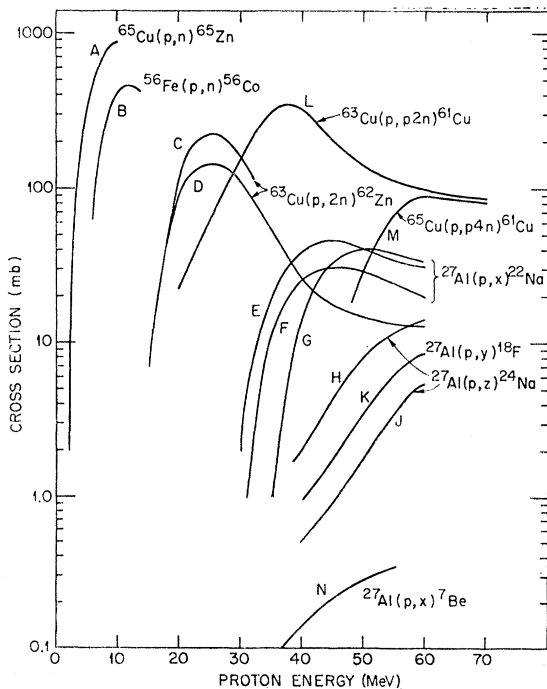


FIG. 3. Excitation functions as reported in the literature (Refs. 9-12) for proton-induced reactions that produce radioactivities in Al, Fe and Cu.

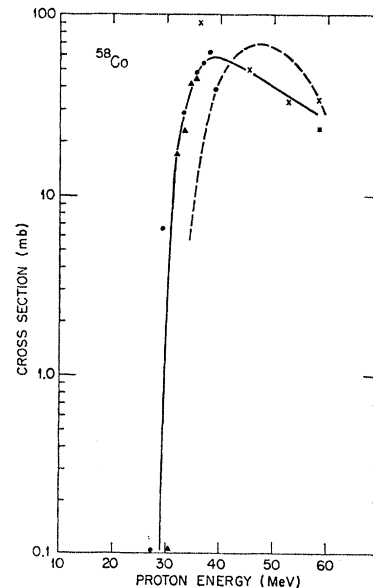


FIG. 4. Excitation function for the production of 71-day ^{58}Co by protons incident on natural iron. The abscissa gives the bombarding energy in laboratory coordinates. The different symbols indicate separate sets of data. The dotted curve shows the evaporation theory prediction for nuclear parameters $r_0=1.5$ and $a=3$.

¹³ J. H. E. Mattauch, W. Thiele, and A. H. Wapstra, Nucl. Phys. 67, 1 (1965).

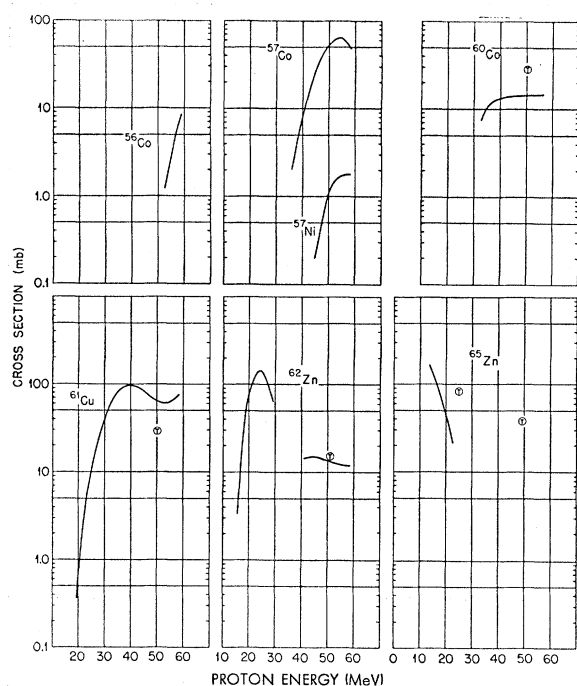


FIG. 5. Excitation functions for the production of 7 radioactive isotopes by bombardment of natural copper. Proton energies are in laboratory coordinates. The encircled T's give a theoretical prediction (see text).

ing with natural copper. Probable errors of $\pm 30\%$ are ascribed. The isotope labelled on each curve is the one whose radiations were measured (the actual γ rays are listed in Table I), but may include the cross-section for the production of shorter lived precursors in a decay chain. For example, experimental difficulties prevented separate measurements of 6 day ^{56}Ni and 77 day ^{56}Co which are produced in the reaction-decay chain $^{63}\text{Cu}(p, \alpha n)^{56}\text{Ni} \rightarrow ^{56}\text{Co} + \beta^+$. In addition, it is possible that hitherto undiscovered ^{56}Cu exists with a very short half-life and a sufficiently low threshold energy that it too is produced and contributes by decay to the ^{56}Co . The same may be true for many of the other cross section measurements. For the mass number 57, however, it was possible to measure the activities of ^{57}Ni and ^{57}Co because of their widely differing half-lives and γ -ray energies.

The excitation function for the production of ^{61}Cu up to ~ 50 MeV shows a shape characteristic of a compound nucleus type reaction.¹⁴ The curve extends to an energy below the minimum threshold (29.3 MeV) for the production of ^{61}Cu by protons incident on ^{63}Cu ; that portion of the cross section is probably largely due to protons interacting with ^{63}Cu . Above 53 MeV the cross section for ^{63}Cu production shows a second rise; probably because the $^{65}\text{Cu}(p, x)^{61}\text{Cu}$ reactions are more probable in this energy region than $^{63}\text{Cu}(p, x)^{61}\text{Cu}$ reactions.¹⁵ Comparison of the excitation function for pro-

¹⁴ S. N. Ghoshal, Phys. Rev. **80**, 939 (1950).

¹⁵ J. W. Meadows, Phys. Rev. **91**, 885 (1953).

TABLE II. List of reactions that involve the largest numerical Q value to produce the radionuclide identified. The Q values are calculated from the 1964 Atomic Mass Table of Mattauch, *et al.*, (Ref. 13).

Target: ^{27}Al (100%)	Q value in lab coordinates (MeV)
Reaction	
$^{27}\text{Al}(p, ^7\text{Be})^{21}\text{Ne}$	-20.7
$^{27}\text{Al}(p, n5\alpha)^7\text{Be}$	-25.8
$^{27}\text{Al}(p, d2\alpha)^{18}\text{F}$	-20.6
$^{27}\text{Al}(p, \alpha d)^{22}\text{Na}$	-21.0
$^{27}\text{Al}(p, d2p)^{24}\text{Na}$	-30.3
Target: ^{54}Fe (5.8%), ^{56}Fe (91.7%), ^{57}Fe (2.2%)	
$^{56}\text{Fe}(p, n2\alpha)^{48}\text{V}$	-22.1
$^{54}\text{Fe}(p, \alpha^2\text{He})^{48}\text{V}$	-22.2
$^{56}\text{Fe}(p, \alpha 2n)^{48}\text{Cr}$	-44.5
$^{56}\text{Fe}(p, \alpha d)^{51}\text{Cr}$	-17.7
$^{54}\text{Fe}(p, \alpha)^{51}\text{Mn}$	+ 3.2
$^{56}\text{Fe}(p, \alpha 2n)^{51}\text{Mn}$	-36.8
$^{54}\text{Fe}(p, d n)^{52}\text{Fe}$	-22.2
$^{56}\text{Fe}(p, d 3n)^{52}\text{Fe}$	-43.3
$^{56}\text{Fe}(p, \alpha n)^{52}\text{Mn}$	-13.3
$^{56}\text{Fe}(p, ^3\text{He})^{54}\text{Mn}$	-17.5
$^{54}\text{Fe}(p, \gamma)^{55}\text{Co}$	+ 5.2
$^{56}\text{Fe}(p, 2n)^{55}\text{Co}$	-15.7
$^{56}\text{Fe}(p, n)^{56}\text{Co}$	- 5.5
Target: ^{63}Cu (69.1%), ^{65}Cu (30.9%)	
$^{63}\text{Cu}(p, \alpha n)^{56}\text{Co}$	-28.1
$^{65}\text{Cu}(p, \alpha 3n)^{56}\text{Co}$	-46.2
$^{63}\text{Cu}(p, \alpha 4n)^{56}\text{Ni}$	-39.7
$^{65}\text{Cu}(p, \alpha 6n)^{56}\text{Ni}$	-55.9
$^{63}\text{Cu}(p, \alpha 3n)^{57}\text{Ni}$	-29.3
$^{65}\text{Cu}(p, \alpha 5n)^{57}\text{Ni}$	-47.4
$^{63}\text{Cu}(p, \alpha t)^{57}\text{Co}$	-16.6
$^{65}\text{Cu}(p, \alpha t 2n)^{57}\text{Co}$	-34.6
$^{63}\text{Cu}(p, \alpha d)^{58}\text{Co}$	-14.2
$^{65}\text{Cu}(p, \alpha t n)^{58}\text{Co}$	-26.0
$^{63}\text{Cu}(p, d 2p)^{60}\text{Co}$	-24.7
$^{65}\text{Cu}(p, \alpha d)^{60}\text{Co}$	-14.1
$^{63}\text{Cu}(p, t)^{61}\text{Cu}$	-11.4
$^{65}\text{Cu}(p, t 2n)^{61}\text{Cu}$	-29.5
$^{63}\text{Cu}(p, 2n)^{62}\text{Zn}$	-13.8
$^{65}\text{Cu}(p, 4n)^{62}\text{Zn}$	-31.4
$^{65}\text{Cu}(p, n)^{65}\text{Zn}$	- 0.3

duction of ^{61}Cu in Fig. 5 with curve L of Fig. 3 shows a discrepancy of a factor of ~ 2 . Part of this is removed if the isotopic abundance of ^{63}Cu is taken into account in making the comparison.

The cross section for the production of ^{62}Zn shows a variation with energy from 15 to 30 MeV which is characteristic of an evaporation type reaction. The threshold for the $^{63}\text{Cu}(p, 2n)$ reaction is 13.8 MeV. The values of the cross section are in agreement (within experimental errors) with those of Ghoshal¹⁴ and Meadows.¹⁵ Above the gap (arising from a malfunction of certain magnetic equipment) in our data from 30 to 40 MeV it is energetically possible for ^{62}Zn to be produced in the reaction $^{65}\text{Cu}(p, 4n)$. Again our data is in essential agreement with previous measurements.¹⁵

An appreciable cross section for production of ^{64}Cu

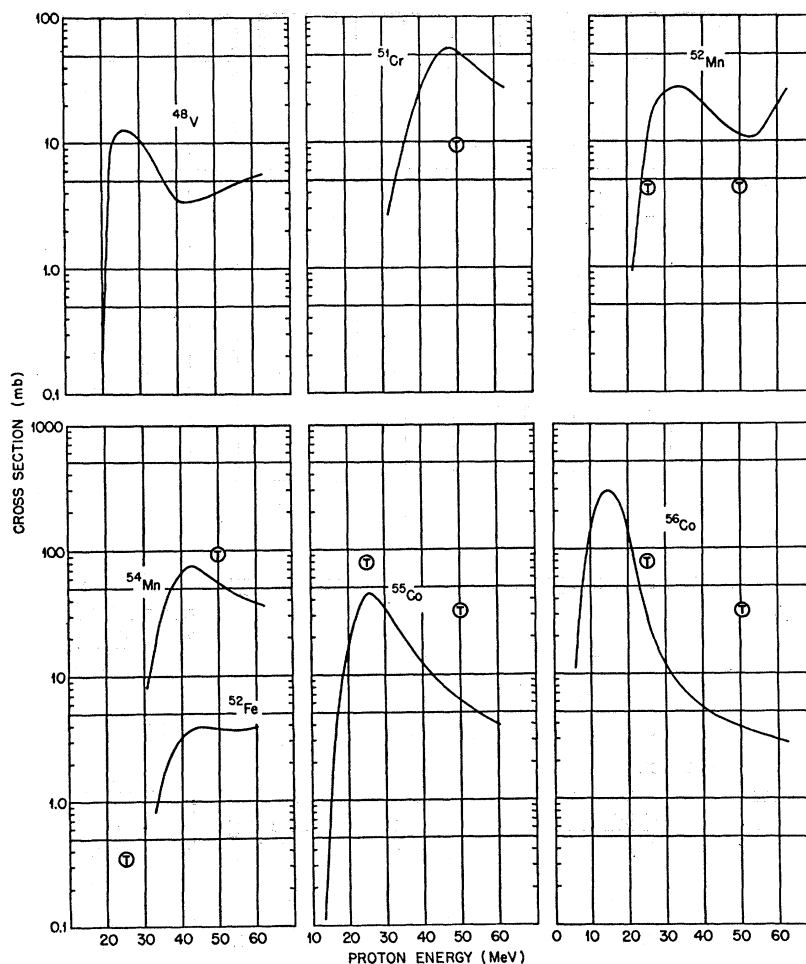


FIG. 6. Excitation functions for the production of 7 radioactive isotopes by proton bombardment of iron. The encircled T's give a theoretical prediction (see text).

by $^{65}\text{Cu}(p,pn)$ reaction has been observed in previous work that employed geiger counters to detect positrons.⁹ In the work reported here, however, ^{64}Cu was not identified in the γ spectra because the only unique γ ray has a very small (0.6%) branching ratio.

In the spectra from copper we identified a previously unreported¹⁶ γ ray with energy 547 ± 3 keV; this was ascribed to the decay of ^{62}Zn on the basis of the same 9.3-h half-life, threshold energy, and excitation function shape as the 590-keV γ ray of ^{62}Zn . The intensity of the 547-keV γ ray was found to be 0.62 ± 0.08 of that of the 590-keV γ ray.

Figure 6 shows excitation functions for the production of seven identified radionuclides in iron. The curves for the $^{56}\text{Fe}(p,n)^{56}\text{Co}$ and $^{56}\text{Fe}(p,2n)^{55}\text{Co}$ are typical of single evaporations of one and two neutrons respectively. The excitation function for the production of ^{48}V shows a broad peak with a second rise at higher bombarding energies. This is because the correspondingly large nuclear excitation permits different nuclear clus-

ters to be emitted. Likewise for ^{52}Mn the prominent peak gives way to a valley at higher energies. The evaporation theory,¹⁷ predicts this effect. In addition, above 4.3 MeV, production of ^{52}Fe in the reaction $^{56}\text{Fe}(p,d3n)$ becomes energetically feasible.

With decreasing energy all but one of excitation functions drops toward zero cross section at the minimum thresholds for their production by protons colliding with the principle iron isotope. The exception is for the production of ^{52}Fe , some of which must be produced by reactions in the 5.8% abundant ^{54}Fe because the threshold for the reaction $^{54}\text{Fe}(p,dn)$ is as low as 22.2 MeV.

Proton bombardment of aluminum foils yielded excitation function data for ^{18}F , ^{22}Na and ^{24}Na ; these are plotted in Fig. 7. The upper portion of the ^{18}F curve is dotted because that data was obtained with a different spectrometer and only the shape of the curve was measured. The curve was then normalized with the data obtained below 50 MeV. Our data yield a measurement of

¹⁶ Since reported by K. I. Roulston of University of Manitoba (private communication).

¹⁷ I. Dostrovsky, Z. Fraenkel, and G. Friedlander, Phys. Rev. **116**, 683 (1959).

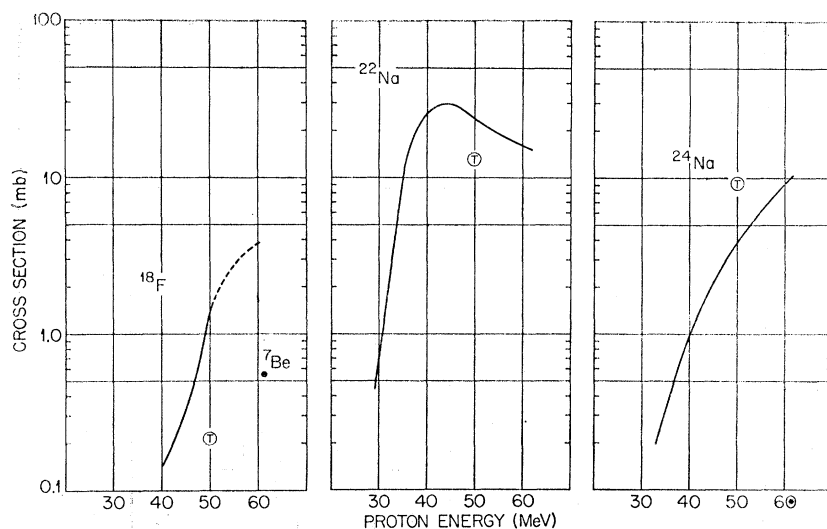


FIG. 7. Excitation functions for the production of 3 radioactive isotopes by protons incident on aluminum. The cross section for the production of ${}^7\text{Be}$ at 60 MeV is also recorded. The encircled T's give a theoretical prediction (see text).

the cross section for the production of ${}^7\text{Be}$ at one energy only.

IV. COMPARISON OF THEORY AND EXPERIMENT

The experimental data were compared with predictions of a cascade-evaporation theory developed by Bertini.¹⁸ The statistical theory assumes a two-stage mechanism in which an incident proton, after entering the nucleus, collides with individual nucleons precipitating an internucleon cascade. Some nucleons may recoil out of the nucleus. When the internal energy is distributed throughout the nuclear volume, evaporation of nucleons, deuterons, tritons, helium-3 nuclei, or α particles can occur. A computer program was used to

predict the cross sections at 25 and 50 MeV; the results are plotted as the encribed letter T on Figs. 5, 6, and 7. Similar comparison was made in the proton bombardment of carbon and reported by the authors in a previous publication.³ Agreement is reasonably good and at the very worst an order of magnitude discrepancy between theory and experiment is found. Lack of perfect agreement is not surprising because the proton bombarding energies are lower than that for which the cascade-evaporation theory is most applicable.

The experimental data were also compared with a theory of nuclear evaporation due to Dostrovsky, Fraenkel and Friedlander.¹⁷ A Monte Carlo code¹⁹ written in FORTRAN and modified for the ORNL CDC-1604A computer, was used to perform the calculations. In this manner theoretical excitation functions were obtained for all the radioisotopes produced and compared with experiment. In most cases good agreement was obtained in the shape and magnitude. An exception to this was in the case of the production of ${}^7\text{Be}$ by protons on carbon³ where the theory predicted a broad peak in the excitation curve with maximum value of the cross section 30 times greater than the experimental value. This lack of agreement for carbon is to be expected because a nucleus with only 13 nucleons has too little resemblance to a liquid drop for the theory to be applicable.

In the statistical evaporation theory two parameters were adjusted. One was the parameter a of the Weisskopf-level-density²⁰ formula

$$W(E) = C \exp[2(aE)^{1/2}].$$

This level-density parameter was taken to be proportional to the mass number of the compound nucleus, $a = A/\gamma$. The best agreement between theory and experiment was found when a was within the approximate

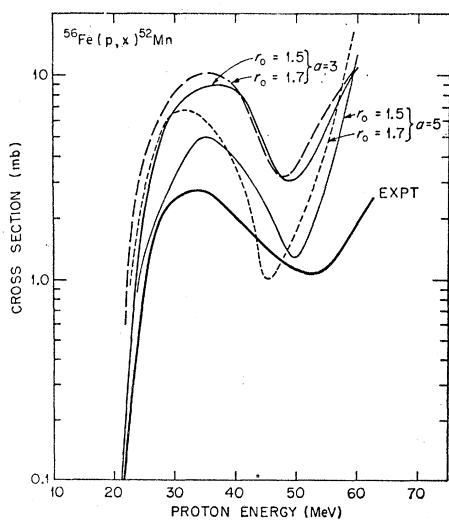


FIG. 8. Comparison of the excitation functions obtained by experiment and from theory (Ref. 17) with the parameters indicated.

¹⁸ H. W. Bertini, Phys. Rev. **131**, 1801 (1963); **138A**, 2 (1965).

¹⁹ P. C. Rogers, Ph.D. thesis, Massachusetts Institute of Technology, 1962 (unpublished).

²⁰ V. F. Weisskopf, Phys. Rev. **52**, 295 (1937).

limit, $3 < a < 5$ for the Al, Fe and Cu targets. Almost invariably the theoretical cross sections increased with a as expected.

The second parameter varied was r_0 , which appears in the formula for the radius, $r = r_0 A^{1/3}$ F. Calculations were made for a nuclear radius parameter of 1.5 F and then 1.7 F. In general, the use of the latter value resulted in larger predicted cross sections and a shifting of peak positions to lower energies. The dashed curve of Fig. 4 shows the excitation function calculated from the compound nucleus theory using the parameter $r_0 = 1.5$ and $a = 3.0$. Fig. 8 makes a comparison between experi-

ment and the evaporation theory with four choices of the parameters.

ACKNOWLEDGMENTS

The authors wish to acknowledge the invaluable assistance of Miss Mavis George in processing much of the data and of Dr. R. L. Hahn who introduced us to the FORTRAN program for making nuclear-evaporation calculations. Also thanks are due to the operating staff of the Oak Ridge Isochronous Cyclotron for their cooperation.

Analysis of the $\text{Ca}^{40}(d,p)\text{Ca}^{41}$ Reaction

S. T. BUTLER, R. G. L. HEWITT, AND J. S. TRUELOVE

Department of Theoretical Physics, University of Sydney, Sydney, New South Wales, Australia

(Received 8 June 1967)

The method recently developed by Butler, Hewitt, McKellar, and May (BHMM) is used in an analysis of the $\text{Ca}^{40}(d,p)\text{Ca}^{41}$ ground-state reaction for six different deuteron energies. The BHMM expression for the (d,p) differential cross section depends only on neutron and proton elastic-scattering wave functions. In the present work, these are generated by optical parameters so chosen as to give elastic-scattering cross sections in satisfactory agreement with experiment. The (d,p) angular distributions are then also found to be in good agreement with experiment. It is determined that the spectroscopic factor relating to the $\text{Ca}^{40}\text{-Ca}^{41}$ overlap has the value 0.56 ± 0.04 .

1. INTRODUCTION

THE method recently developed by Butler, Hewitt, McKellar, and May¹ (hereafter referred to as BHMM) is used in an analysis of the $\text{Ca}^{40}(d,p)\text{Ca}^{41}$ ground-state reaction for six different deuteron energies.

The BHMM expression for the (d,p) differential cross section depends only on neutron and proton elastic-scattering wave functions. In the present work, these are generated by optical parameters so chosen as to give elastic-scattering cross sections in satisfactory agreement with experiment for both neutrons and protons at appropriate energies.

The averaged parameter set of Perey and Buck² for neutron scattering and that of Buck³ for proton scattering are chosen as a starting point. It is found that these parameters will generate elastic-scattering cross sections in consistent agreement with experiment for scattering on Ca^{40} with two simple modifications:

(a) The surface diffuseness parameters (a, b) must be reduced to $(a\lambda, b\lambda)$ with $\lambda = 0.80$, for both neutron and proton sets. This presumably reflects the fact that the Ca^{40} nucleus has a somewhat sharper surface than average nuclei.

(b) The strengths W_N, W_P of the imaginary optical

potentials for neutron and proton scattering must in general be altered from the averaged values. For neutrons, we find $W_N = 5.4$ MeV is required for 6-MeV scattering and $W_N = 7.0$ MeV for 14-MeV scattering. For protons, we find $W_P = 6.0$ MeV for 14.6-MeV scattering and $W_P = 7.0$ MeV for 17.3-MeV scattering. In each case we assume a linear interpolation between the two energies.

The BHMM differential cross sections for the $\text{Ca}^{40}(d,p)\text{Ca}^{41}$ reaction are then calculated without further adjustment of these parameters and compared with experiment⁴ at six deuteron energies from 7 to 12 MeV. Agreement is good at all energies. Typical of this agreement are the 12-MeV results shown, together with experimental points, in Fig. 1. The neutron orbital angular momentum is, of course, given by $l = 3$ and the BHMM results of Fig. 1 require a spectroscopic factor $S = 0.60$. (It is to be noted that the less accurate value obtained in Ref. 1 using simple averaged optical parameters, without heed to elastic scattering, was $S \approx 0.5$).

For comparison purposes we also show the results of corresponding distorted-wave Born analysis (DWBA) made by Lee, Schiffer, Zeidman, Satchler, Drisko, and Bassel⁴ at each energy, the comparison at 12 MeV being shown in Fig. 1. It is found that the BHMM and DWBA angular distributions are in comparable agreement with

⁴L. L. Lee, J. P. Schiffer, B. Zeidman, G. R. Satchler, R. M. Drisko, and R. H. Bassel, *Phys. Rev.* **136**, B971 (1964).

¹S. T. Butler, R. G. L. Hewitt, B. H. J. McKellar, and R. M. May, *Ann. Phys. (N. Y.)* **23**, 282 (1967).

²F. Perey and B. Buck, *Nucl. Phys.* **32**, 353 (1962).

³B. Buck, *Phys. Rev.* **130**, 712 (1963).